Electronic Supplementary Material (ESI) for Journal of Materials Chemistry A.

Electronic Supplementary Information

Hydrazine-assisted formation of ultrathin MoS_2 nanosheets for enhancing their co-catalytic activity in photocatalytic hydrogen evolution

*D. Amaranatha Reddy, Hanbit Park, Sangyeob Hong, D. Praveen Kumar and Tae Kyu Kim**

Department of Chemistry and Chemical Institute for Functional Materials, Pusan National University, Busan 46241, Republic of Korea

* Corresponding Author. E-mail) tkkim@pusan.ac.kr

1. EXPERIMENTAL SECTION

1.1 Reagents:

$Cd(CH_3COO)_2 \cdot 2H_2O$ (98%), $Na_2MoO_4 \cdot 2H_2O$ (99%), CH_4N_2S (99 %) and lactic acid were obtained from DAEJUNG Chemicals, South Korea. The bulk MoS_2 (99 %), C_2H_5NS (98 %), Hydrazine were obtained from Alfa Aesar, South Korea.

1.2 Synthesis of T-MoS_2 nanosheets:

Thick MoS_2 (T-MoS_2) nanosheets were synthesized via a hydrothermal method. A typical synthetic process involved dissolving Na_2MoO_4, (0.3 g) and C_2H_5NS (0.6 g) at the required stoichiometry into de-ionized (DI) water in a Teflon-lined autoclave. After stirring for 3 h, the autoclave was placed inside a furnace and heated at 200 °C for 24 h. After completion of the reaction, the autoclave was air-cooled to room temperature. The products were collected and washed several times with DI water to remove any impurities and then finally dried at 100 °C for 6 h to obtain the final products. The black precipitates were the T-MoS_2 nanosheets, which were synthesized with yield of 0.15 g.

1.3 Synthesis of CdS nanorods

CdS nanorods were synthesized via a hydrothermal method. A typical synthetic process involved dissolving $Cd(CH_3COO)_2 \cdot 2H_2O$ (3.2 mmol), CH_4N_2S (16 mmol) at the required stoichiometry into 60 mL ethylenediamine. After stirring for 2 h, the solution was transformed to 80 ml Teflon-lined autoclave and was placed inside a furnace and heated at 160 °C for 48 h. After completion of the reaction, the autoclave was air-cooled to room temperature. The products were collected and washed several times with DI water to remove any impurities and then finally dried at 100 °C for 6 h to obtain the final products with yield of 0.958 g.

1.4 Synthesis of CdS/T--MoS$_2$ nanocomposites

To synthesize CdS/T-MoS$_2$ nanocomposites, the synthesized CdS and desired wt.% of T-MoS$_2$ (2, 4, 6, 8 and 10) were dispersed in 20 mL of DMF in a separate beaker and both of the samples were stirred for 30 minutes. After stirring, T-MoS$_2$ suspension was mixed with the CdS solution. The mixture was vigorously stirred for 24 h to obtain a homogeneous suspension. After completion of the reaction, the products were collected and washed several times with DI water to remove the impurities and finally dried at 100 °C for 6 h to obtain the final products. CdS/T-MoS$_2$ with different T-MoS$_2$ contents was prepared following the same method with different wt.% of T-MoS$_2$ as the reactant.

1.5 Synthesis of ultrathin MoS$_2$/CdS nanocomposite:

To synthesize CdS/UT-MoS$_2$ nanocomposites, at first the desired wt.% of T-MoS$_2$ (2, 4, 6, 8 and 10) were dispersed in 30 mL of DMF and ultra sonic for 3 h. After sonication for 3 h, the suspension was all black. Then, as-prepared CdS nanorods (50 mg) quickly poured into the former black dispersion. The mixture was subjected to ultrasonic treatment for 1 h followed by overnight stirring to achieve close interfacial contact between UT-MoS$_2$ and CdS nanorods. The UT-MoS$_2$/CdS nanocomposite was collected after removal of DMF by vacuum distillation. The final products were collected and washed several times with ethanol to remove the impurities and finally heated in air at 80 °C for 10 h to obtain the final products.

1.6 Synthesis of hydrazine assisted liquid exfoliation formation of ultrathin- MoS$_2$ (HUT-MoS$_2$)/CdS nanocomposite

To synthesize CdS/HUT-MoS_2 nanocomposites, at first the desired wt.% of T-MoS_2 (2, 4, 6, and 10) were dispersed in 30 mL of DMF and desired volume of hydrazine (0.5, 1, 1.5 and 2 vol.%) and ultra sonic for 3 h. Then, as-prepared CdS nanorods (50 mg) quickly poured into the former dispersion solution. Then the mixture was subjected to ultrasonic treatment for 1 h followed by overnight stirring to achieve close interfacial contact between HUT-MoS_2 and CdS nanorods. The HUT-MoS_2/CdS nanocomposite was collected after removal of DMF by vacuum distillation. The final products were collected and washed several times with ethanol to remove the impurities and finally heated in air at 80 °C for 10 h to obtain the final products.

1.7 Synthesis of bulk- MoS_2/CdS nanocomposites

The commercial bulk MoS_2 nanostructures was purchased from Alfa Aesar, South Korea and used without further purification. To synthesize CdS/B-MoS_2 nanocomposites, the synthesized CdS and desired wt.% of C-MoS_2 (2, 4, 6, 8 and 10) were dispersed in 20 mL of DMF in a separate beaker and both of the samples were stirred for 30 minutes. After stirring, B-MoS_2 suspension was mixed with the CdS solution. The mixture was vigorously stirred for 24 h to obtain a homogeneous suspension. After completion of the reaction, the products were collected and washed several times with DI water to remove the impurities and finally heated in air at 100 °C for 6 h to obtain the final products. CdS/B-MoS_2 with different B-MoS_2 contents was prepared following the same method with different wt.% of B-MoS_2 as the reactant.

1.8 Photo-deposition of Pt nanoparticles on CdS nanorods

The Pt-loaded hybrid particles were prepared using 150-W xenon-arc lamp by photo deposition technique. In detail, 50 mg of above synthesized CdS nanorods are suspended in mixed solvent 20 mL of a mixed solvent H_2O/lactic acid (80:20 v/v)). Then, required stoichiometric amount of $H_2PtCl_6 \cdot 6H_2O$ (1, 2, 3, 4 and 5 wt% of Pt) were added to the above suspension. The solution was then thoroughly degassed and bubbled with Ar for 30 min to remove the air inside and finally irradiated by a 150 W Xe-arc lamp for 2 h. After irradiation, the filtered Pt-loaded CdS nanocomposites were washed with distilled water and ethanol to remove the unnecessary impurities and dried at 80 ^{o}C for 10 h to obtain the final products.

2. Characterization

The morphologies and average particle sizes were measured using a Hitachi S-4800 field emission scanning electron microscope (FESEM) equipped with an Inca 400 energy-dispersive spectrometer from Oxford Instruments. The microstructure properties were measured using a JEOL JEM-2100F transmission electron microscope (TEM) with an accelerating voltage of 200 kV. The atomic force microscopy (AFM) images were obtained by using XE-100 atomic force microscopy. Raman spectra were obtained on an Xper-Ram 200 (Nano Base, Korea) micro Raman spectrometer with a solid-state laser (excitation at 532 nm) at room temperature. Phase determination of the as-prepared powders was performed using a Bruker D8 Advance X-ray diffractometer with a Cu Kα X-ray source. X-ray photoelectron spectroscopy (XPS) was performed using a monochromated Al Kα X-ray source ($h\nu = 1486.6$ eV) at an energy of 15 kV/150 W. The nitrogen adsorption–desorption isotherm measurements for the samples were carried out at 77.35 K using a Tristar 3000 Micromeritics instrument to measure the surface area. The optical absorption measurements were performed using a Shimadzu UV-1800 double-beam spectrophotometer. Photoluminescence (PL) measurements were performed at room temperature using Hitachi F-7000 fluorescence spectrophotometer with an excitation wavelength of 380 nm.

2.1 Photocatalytic hydrogen Production

The photocatalytic hydrogen evolution experiments were performed in a 150 ml quartz beaker at ambient temperature and atmospheric pressure. The openings of the flask were sealed with silicone rubber septum. A solar simulator equipped with an AM 1.5G filter and 150 W Xe lamp (Abet Technologies) was used as the light source. The output light intensity was adjusted to 1 sun (100 W/m^2) using 15151 low-cost calibrated Si reference cell (ABET technologies). Before irradiation, the system was evacuation and bubbled with Ar for 30 min to remove the air inside. The hydrogen gas evolved was determined using an off-line gas chromatograph (Young Lin Autochro-3000, model 4900) equipped with thermal conductivity detector and a 5 Å molecular sieve column. The 100 μL of produced hydrogen gas in headspace of reactor was collected and injected into the GC and calculated by a calibration plot to 5 % standard gas of hydrogen.

The apparent quantum efficiency (QE) was measured according to the equation below

$$QE = \frac{\text{nuber of reacted electrons}}{number\ of\ incident\ photons} \text{ x } 100\ \%$$

$$= \frac{\text{number of evolved } \mathrm{H_2}\text{molecules x 2}}{number\ of\ incident\ photons} \text{x100\%}$$

Here the QE was measured under the same photocatalytic hydrogen evolution experimental conditions except the irradiation source, here 150 W Xe lamp with 425 nm band pass filter were used as light sources, instead of the solar simulator. The output light intensity was measured using 15151 low-cost calibrated Si reference cell (ABET technologies). The liquid level is ~16 cm far from the window of lamp and the illuminated area is 21.24 cm^2.

2.2 Photo-electrochemical measurements

Photo-electrochemical measurements were performed in a three-electrode system using a CHI 617B electrochemical workstation. A solar simulator equipped with an AM 1.5G filter and 150 W Xe lamp (Abet Technologies) was used as the irradiation source to produce monochromatic illuminating light. The output light intensity was adjusted to 1 sun (100 W/m^2) using 15151 low-cost calibrated Si reference cell (ABET technologies). The reference and counter electrodes were Ag/AgCl and platinum wire, respectively, and 0.5 M Na_2SO_4 aqueous solution served as the electrolyte. The measured pH value is 6.72. To prepare the working electrode, the as-synthesized 10 mg of CdS, CdS/T-MoS_2, CdS/UT-MoS_2 and CdS/HUT-MoS_2 nanocomposites were first dispersed into ethanol (450 µl) and 50 µl Nafion mixtures using soft ultrasonic stirring to obtain a uniform suspension. The solution containing the catalyst (30 µl) was dropped onto the pretreated indium–tin oxide (ITO) conductor glass substrate, which was then dried in an oven at 80 °C for 3 h. Photo-responses were measured at 0.0 V during on-off cycling of the solar simulator. Electrochemical impedance spectroscopy (EIS) was carried out at open-circuit potential over the frequency range of 10^5 and 10^{-1} Hz with an AC voltage magnitude of 5 mV. Moreover, to evaluate the flat-band potential (V_{FB}) of the CdS, B-MoS_2, T-MoS_2, UT-MoS_2 and HUT-MoS_2 Mott−Schottky plots at a frequency of 1 kHz were measured using a standard potentiostat equipped with an impedance spectra analyzer in the same electrochemical configuration and electrolyte under the dark condition. The measured potentials versus Ag/AgCl were converted to the normal hydrogen electrode (NHE) scale by $E_{NHE} = E_{Ag/Agcl} + 0.197$. The cyclicvoltammograms (CV) were measured with as scanning rate of 10mV/s using whereas the electrolyte was consisting of 0.1M Na_2SO_4 aqueous solution with 1mM $K_3[Fe(CN)_6]$.

2.3 Detection of $^{\cdot}OH$ radicals:

Formation of hydroxyl radicals ($^{\cdot}OH$) produced on the surface of as-synthesized CdS/WS_2-MoS_2 nanostructures under simulated sunlight irradiation, was detected by the photoluminescence (PL) technique using terephthalic acid (TA) as a probe molecule. For the reaction we taken 10 mg of CdS/WS_2-MoS_2 were dispersed in a 40 mL of the 5×10^{-4} M TA aqueous solution with a concentration of NaOH (2×10^{-3} M) solution at room temperature. The suspension was irradiated by a simulated sunlight irradiation. At every one hour, 5 mL of the suspension was collected and centrifuged for 15 min. Finally PL spectra of generated 2-hydroxyterephthalic acid were measured by a Hitachi F-7000 fluorescence spectrophotometer.

3. Supporting Figures

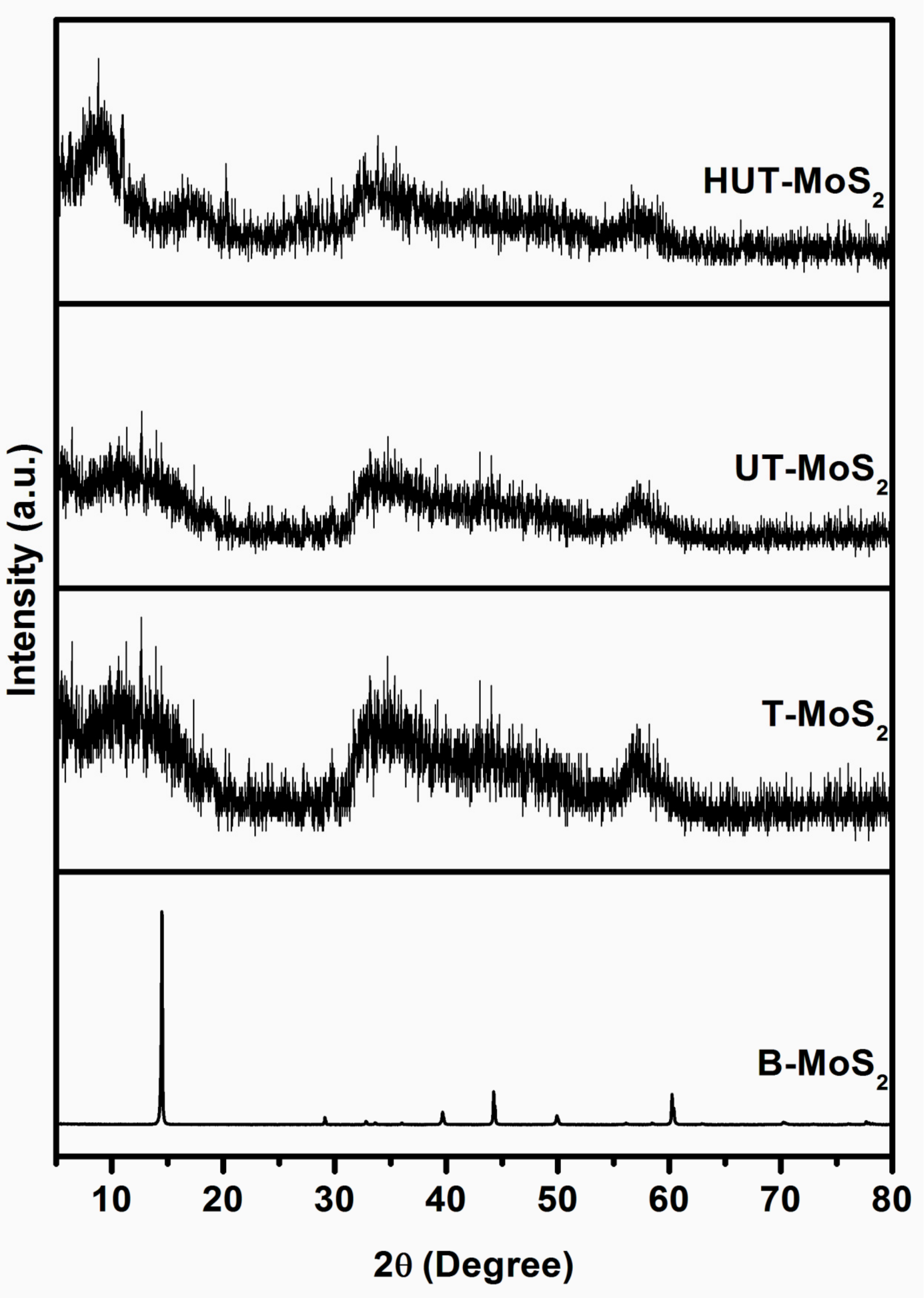

Figure S1. XRD patterns of B-MoS$_2$, T-MoS$_2$, UT-MoS$_2$ and HUT-MoS$_2$ nanostructures.

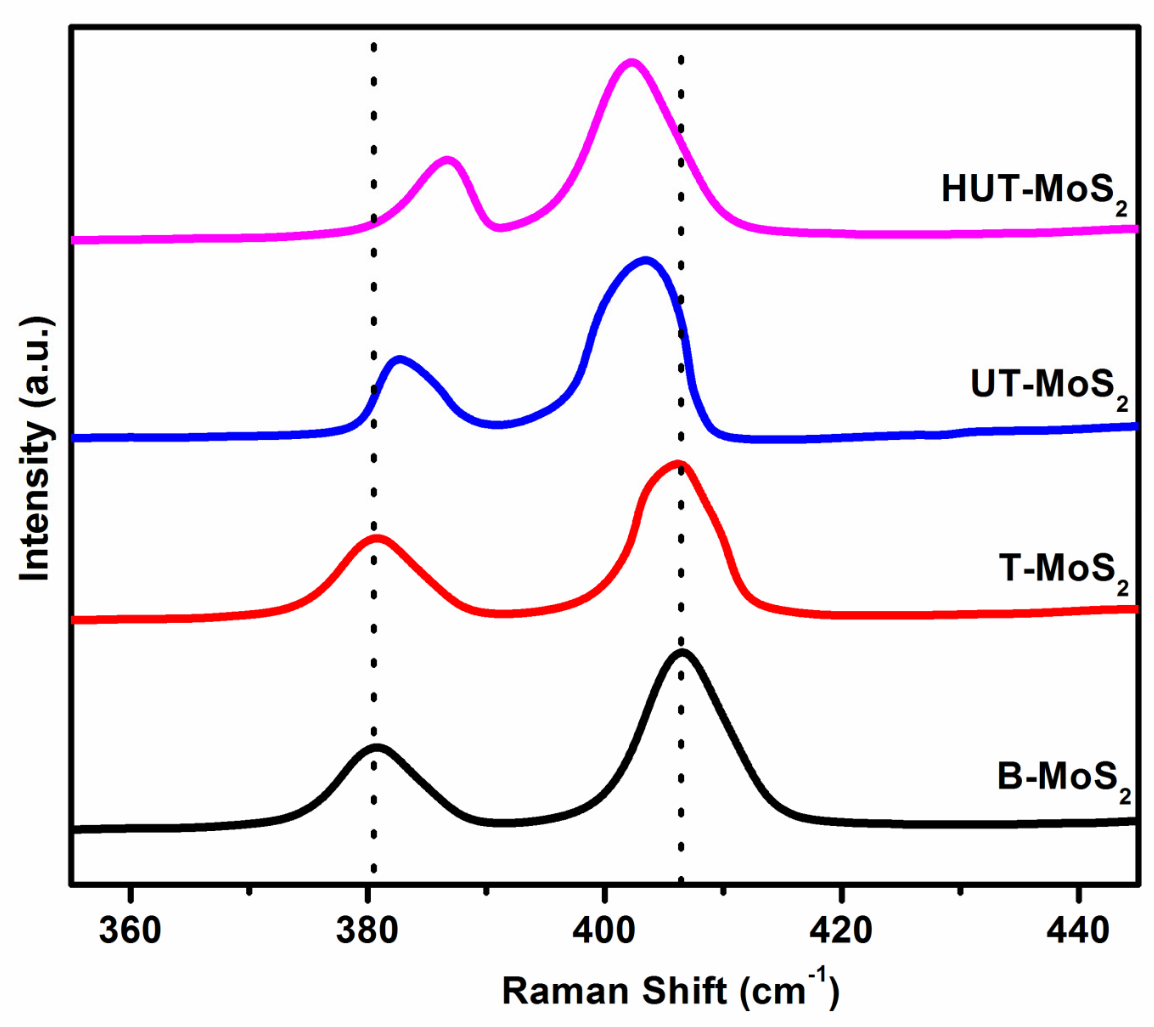

Figure S2. Raman spectra of B-MoS_2, T-MoS_2, UT-MoS_2 and HUT-MoS_2 nanostructures.

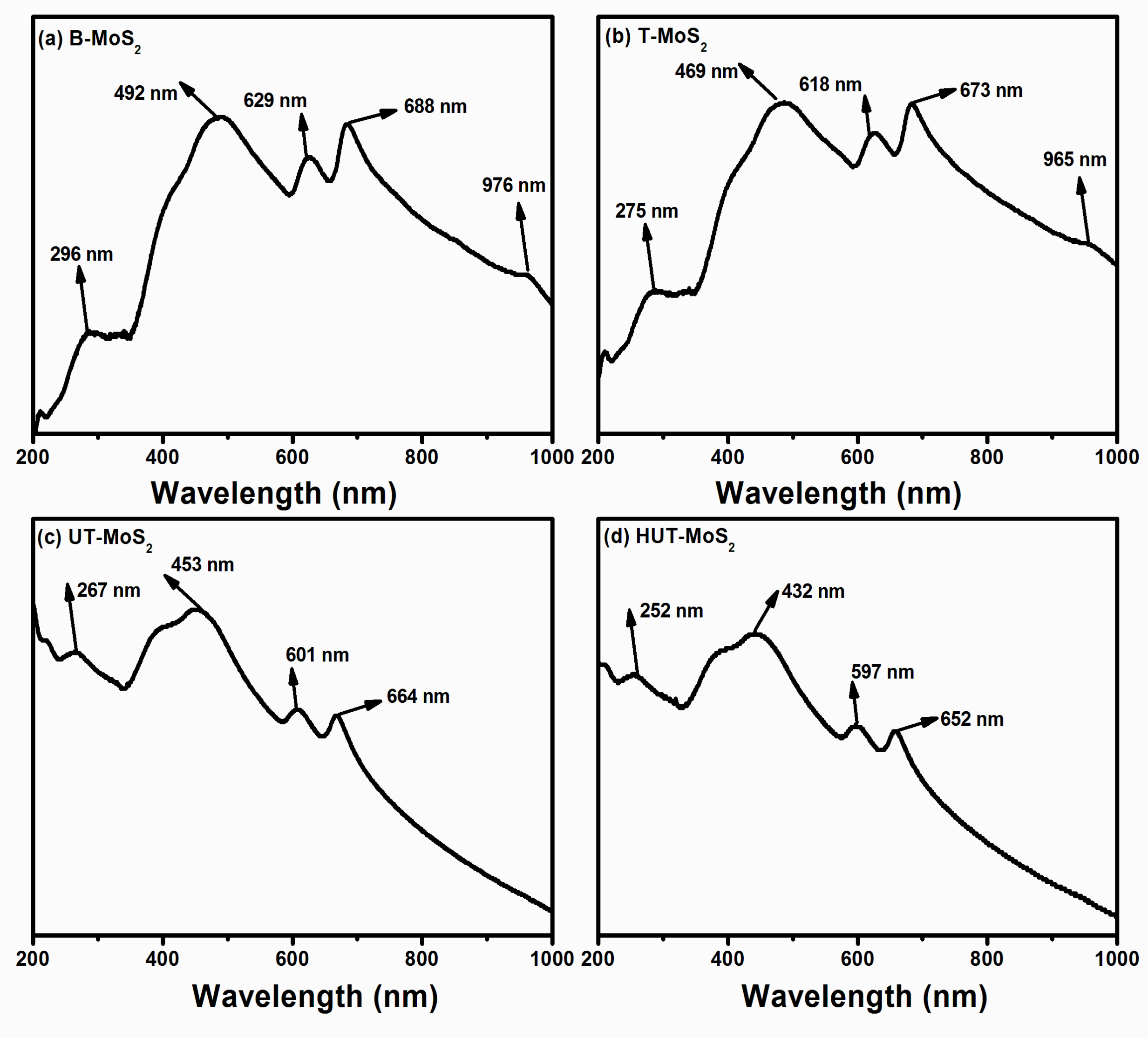

Figure S3. UV-Vis absorption spectra of (a) B-MoS$_2$ (b) T-MoS$_2$ (c) UT-MoS$_2$ and (d) HUT-MoS$_2$ nanostructures.

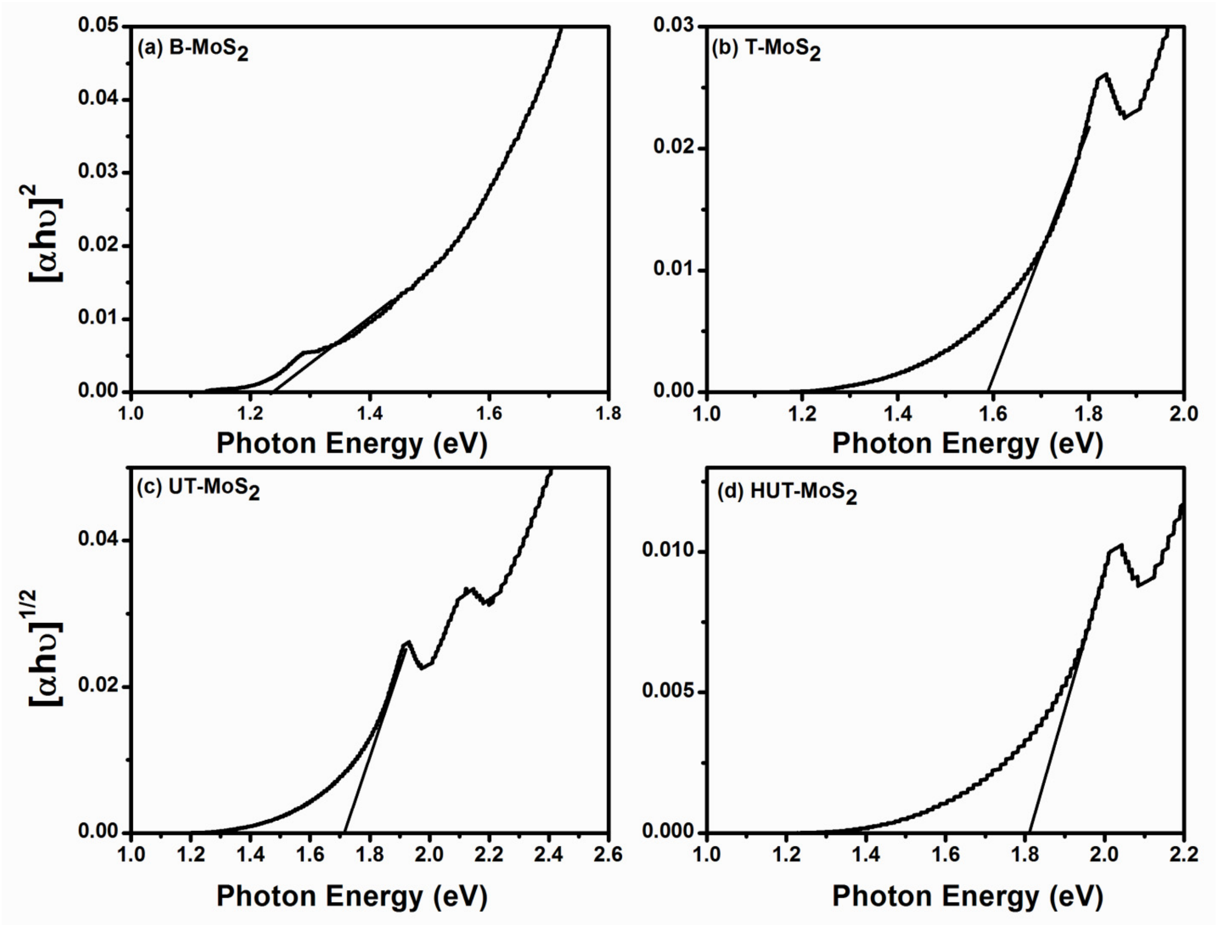

Figure S4. Tauc plots and band gap energy estimation (a) B-MoS_2 (b) T-MoS_2 (c) UT-MoS_2 and (d) HUT-MoS_2 nanostructures.

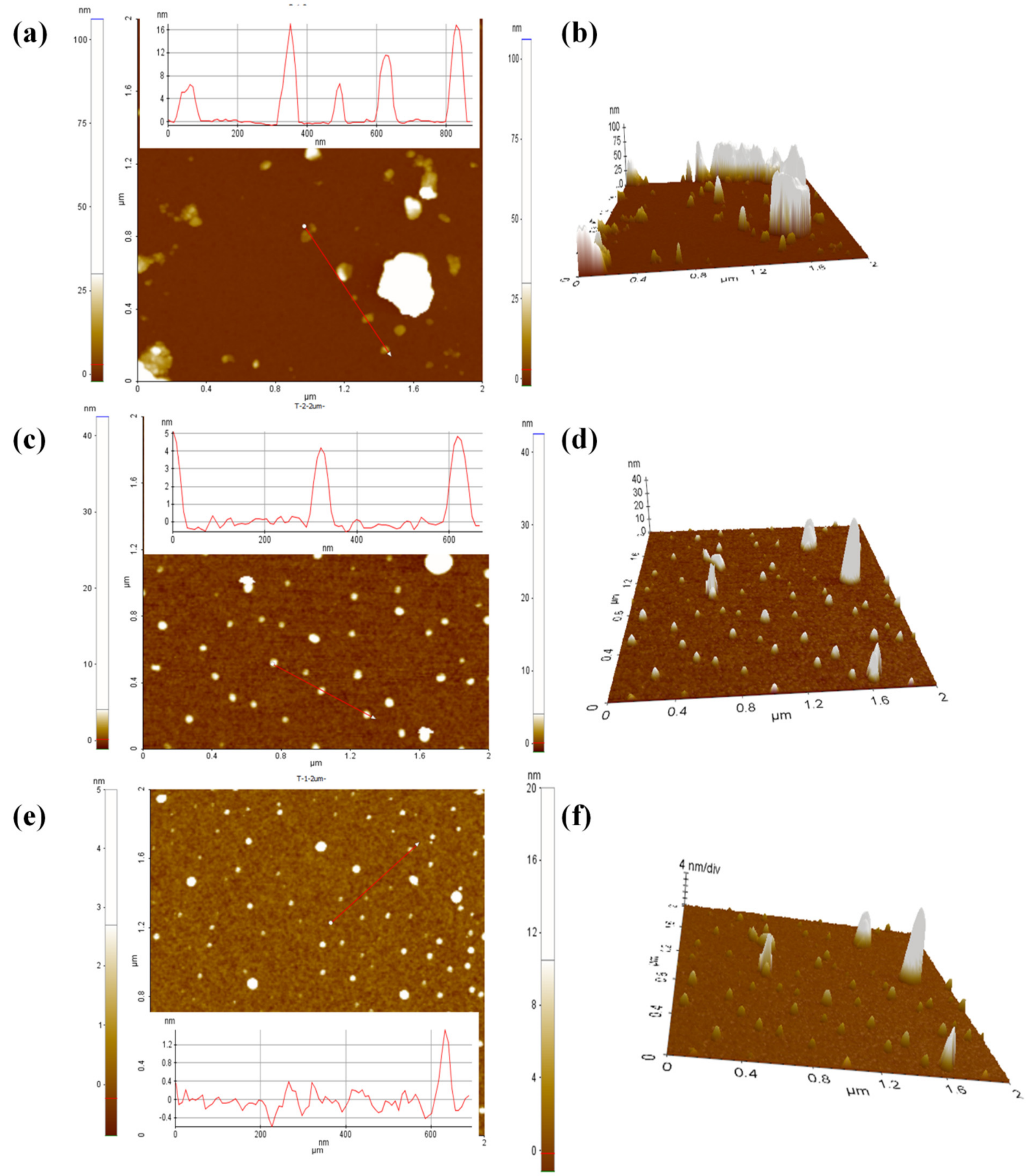

Figure S5. AFM micrographs of 2D, 3D micrographs and corresponding height profiles (a, b) T-MoS$_2$ (c, d) UT-MoS$_2$ and (d) HUT-MoS$_2$ nanostructures.

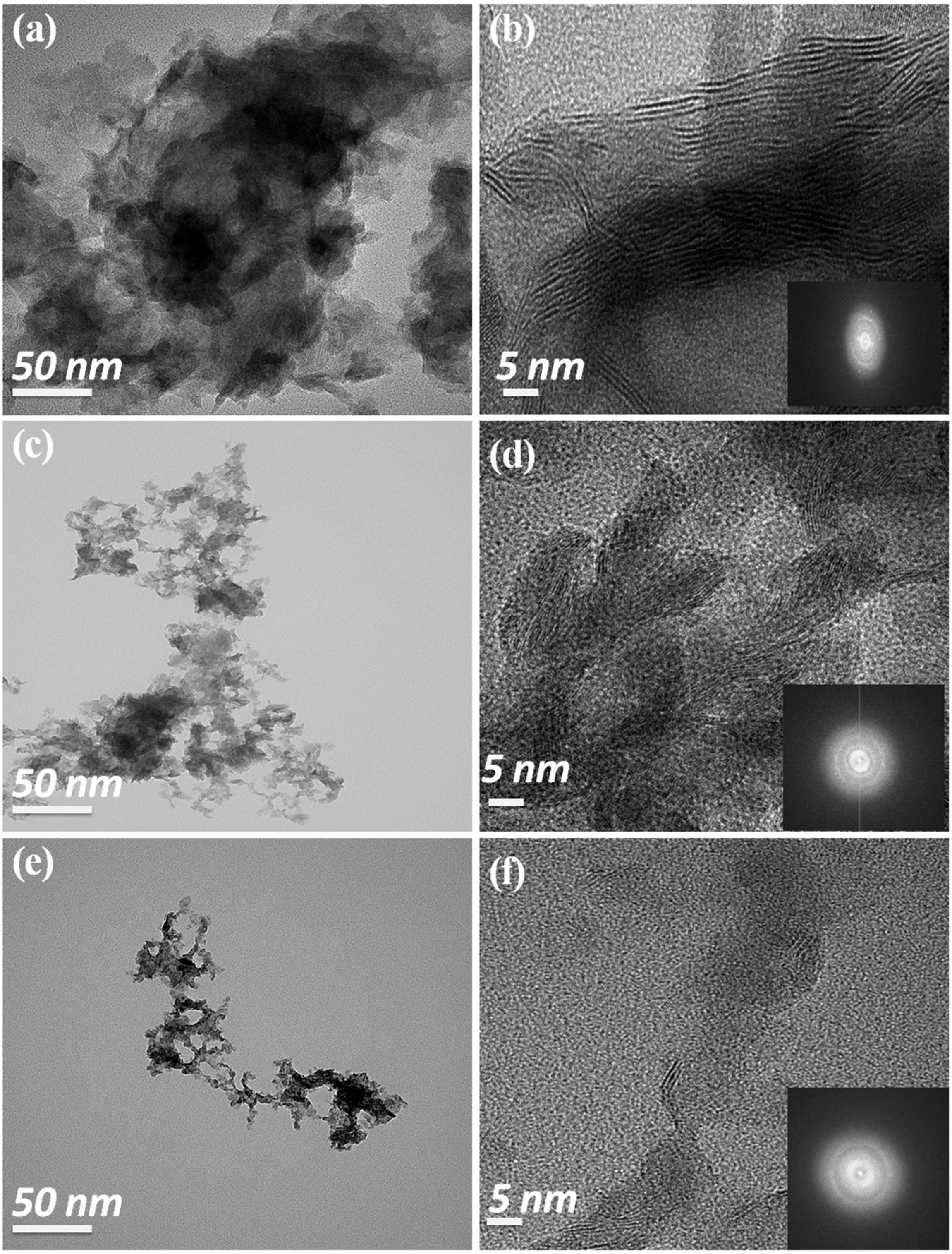

Figure S6. TEM, HRTEM and corresponding SAED patterns of (a, b) B-MoS_2 nanosheets, (c, d) UT-MoS_2 nanosheets, and (e, f) HUT-MoS_2 nanostructures.

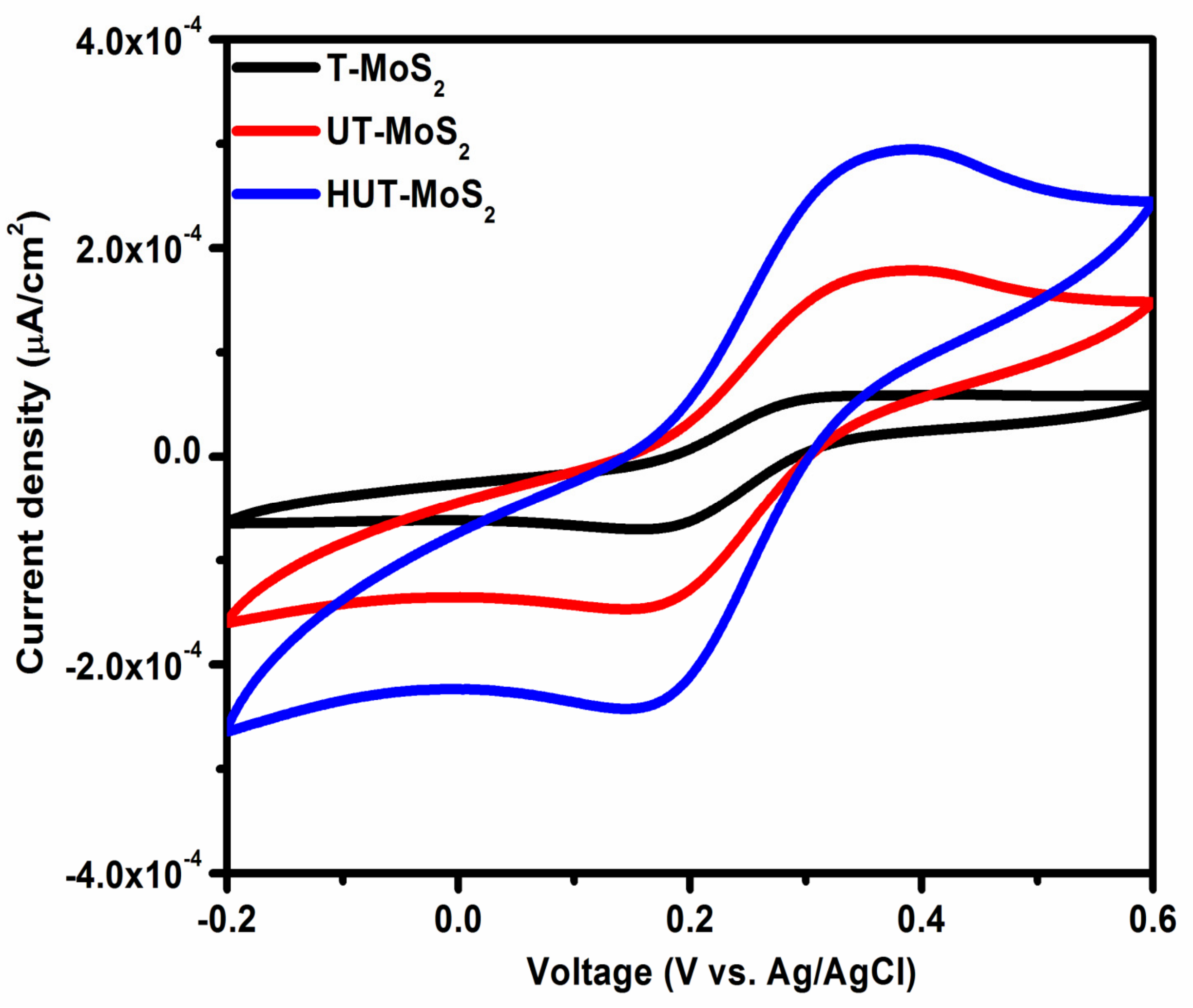

Figure S7. Cyclic voltammograms of the as-synthesized T-MoS_2, UT-MoS_2 and HUT-MoS_2 nanosheets.

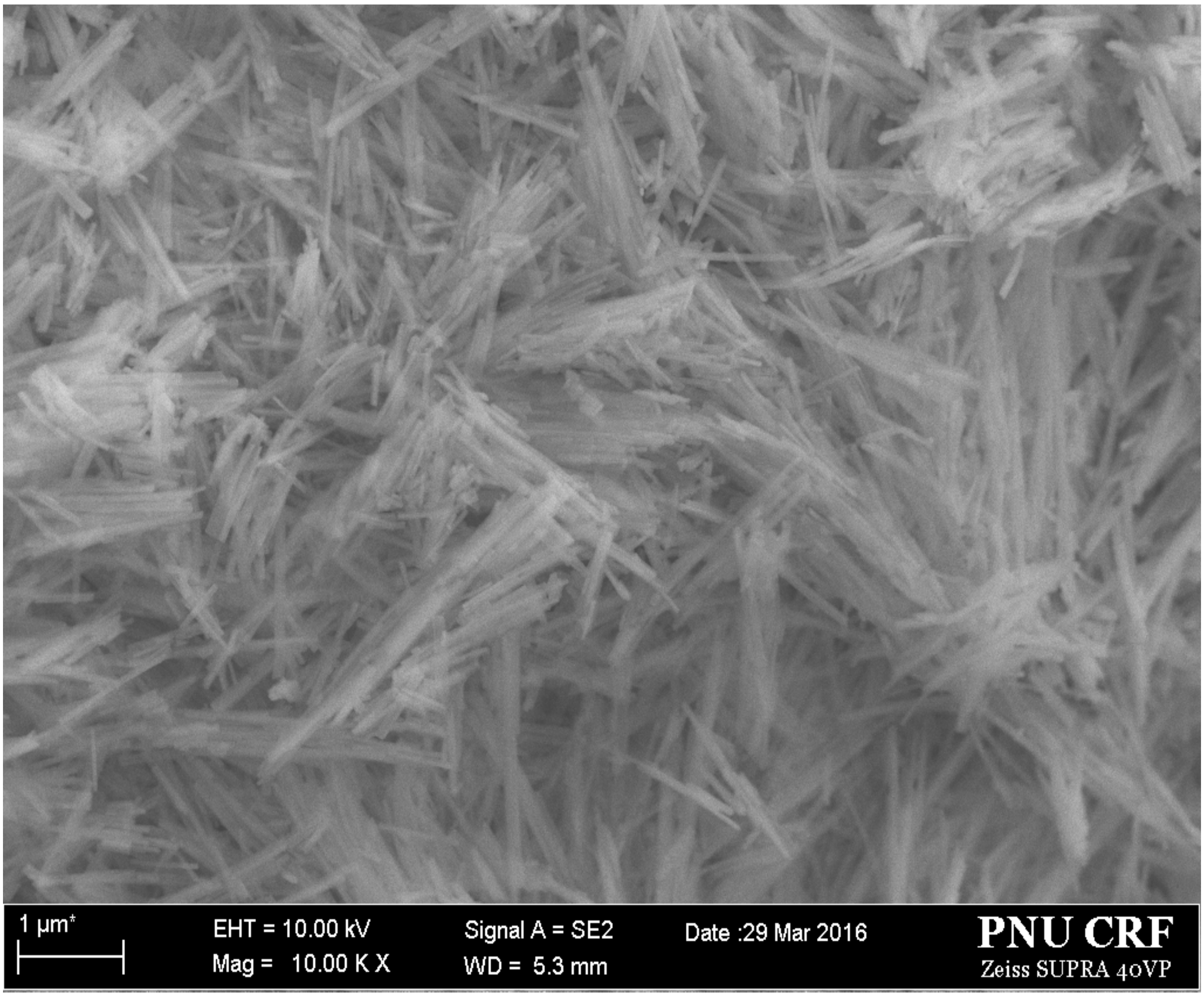

Figure S8. FESEM image of as-synthesized CdS nanostructures.

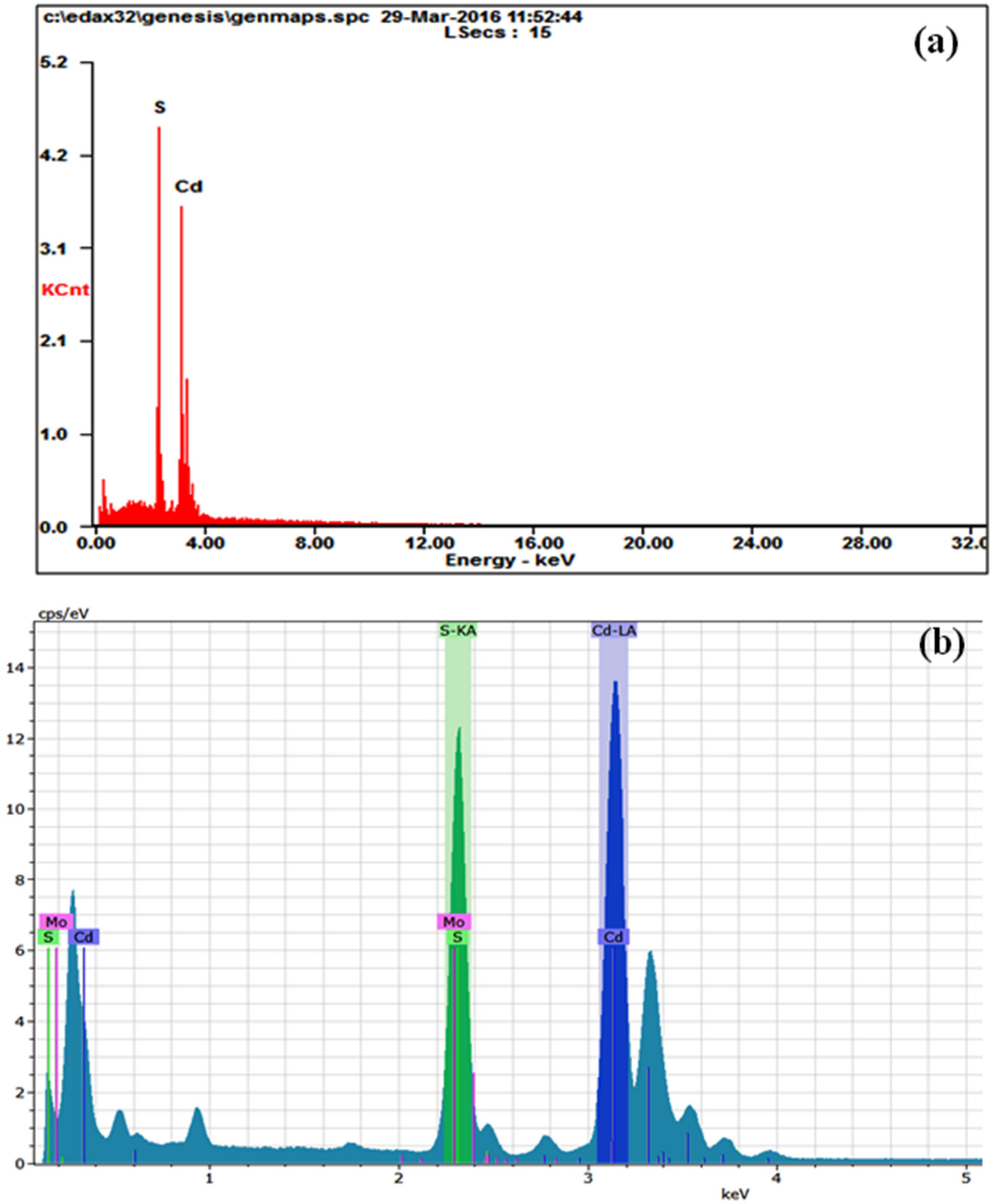

Figure S9. EDS spectra of (a) CdS and (b) CdS/HUT-MoS_2 nanocomposites.

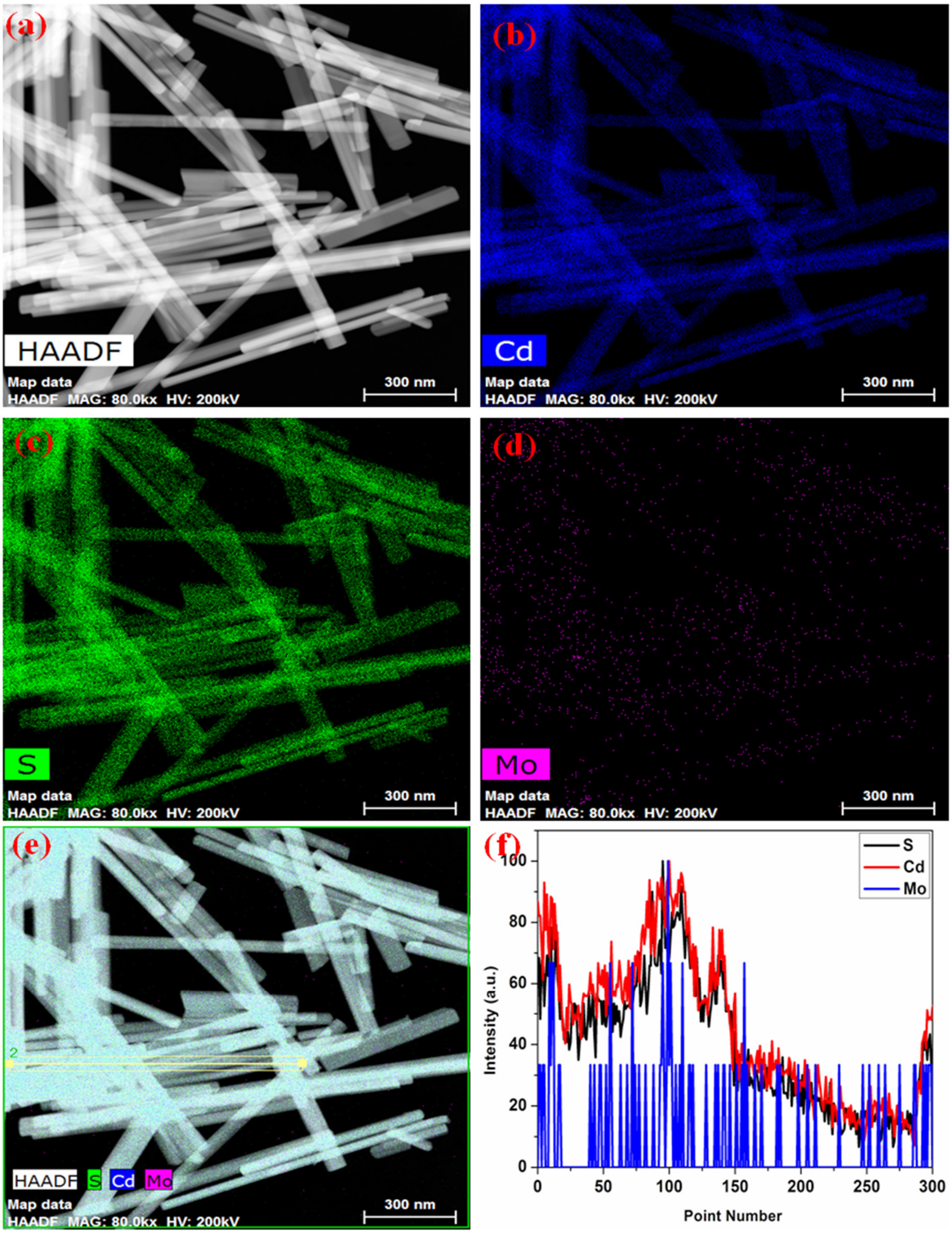

Figure S10. (a) TEM electron micrograph and elemental mapping of CdS/HUT-MoS_2 nanocomposite showing the presence of (b) Cd, (c) S, (d) Mo, and (e) all elements. (f) The line spectrum of all presented elements.

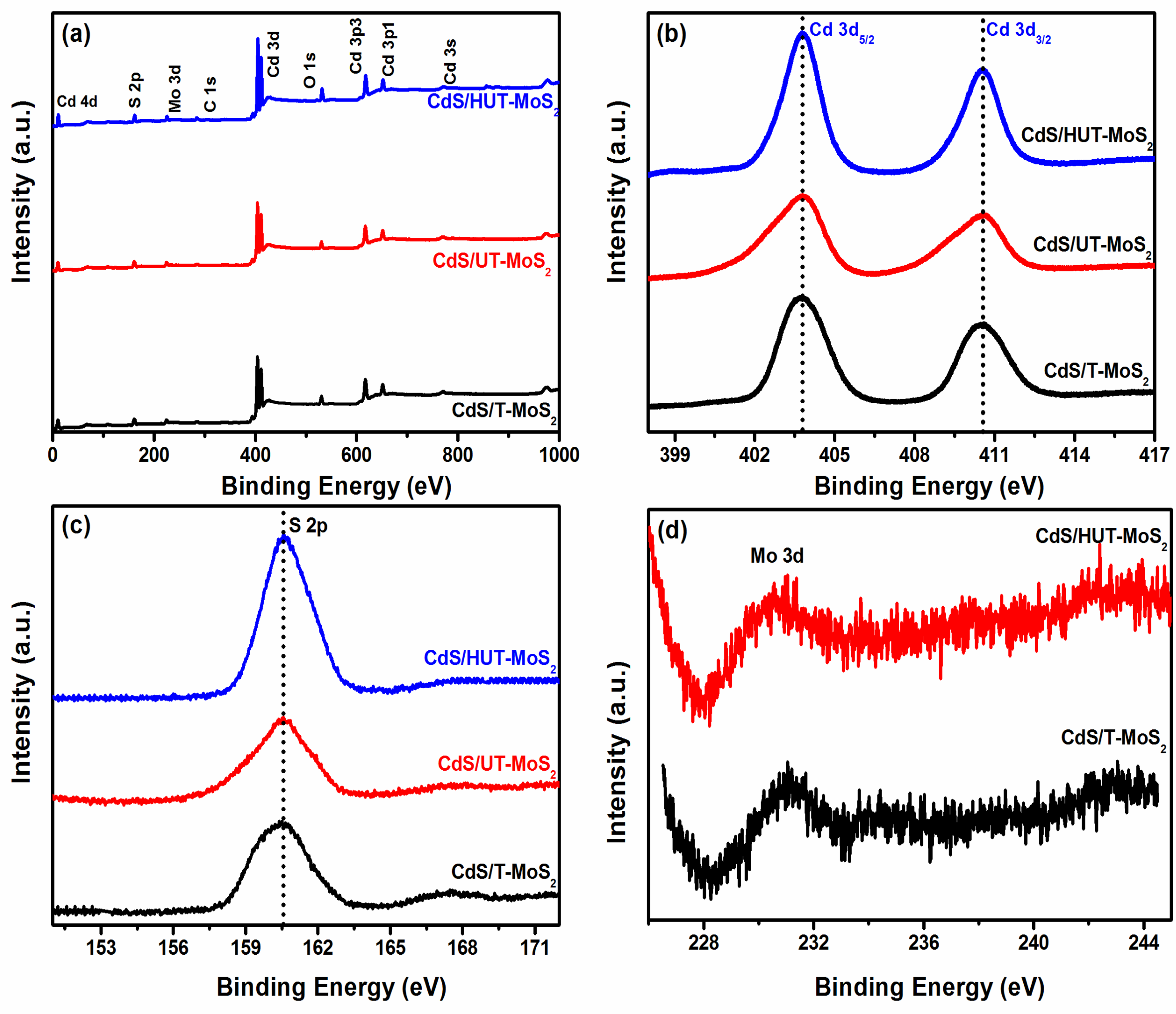

Figure S11. Comparison of XPS survey and narrow XPS spectra of CdS/T-MoS$_2$, CdS/UT-MoS$_2$, and CdS/HUT-MoS$_2$ nanostructures.

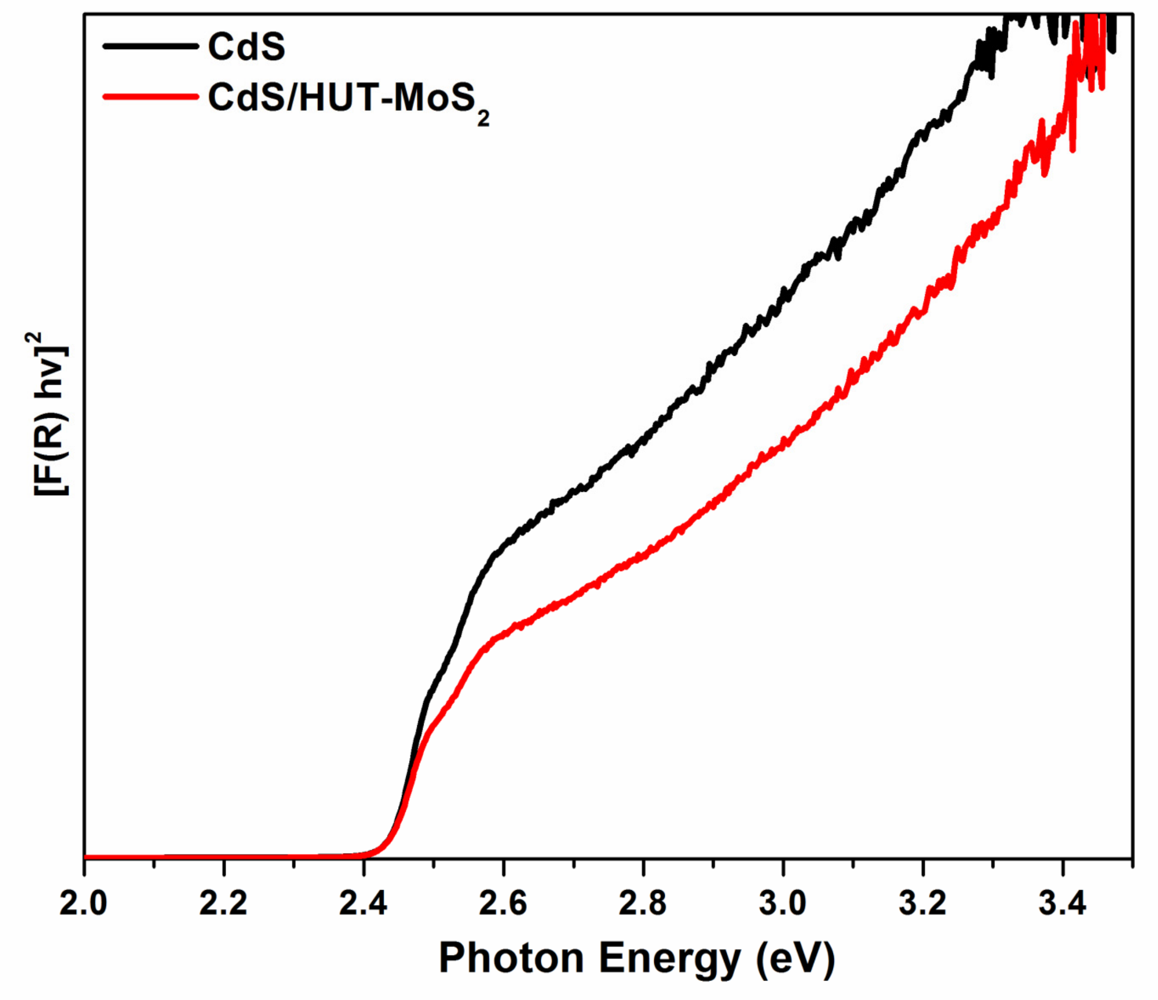

Figure S12. Kubelka–Munk plots of CdS and CdS/HUT-MoS_2 nanocomposite.

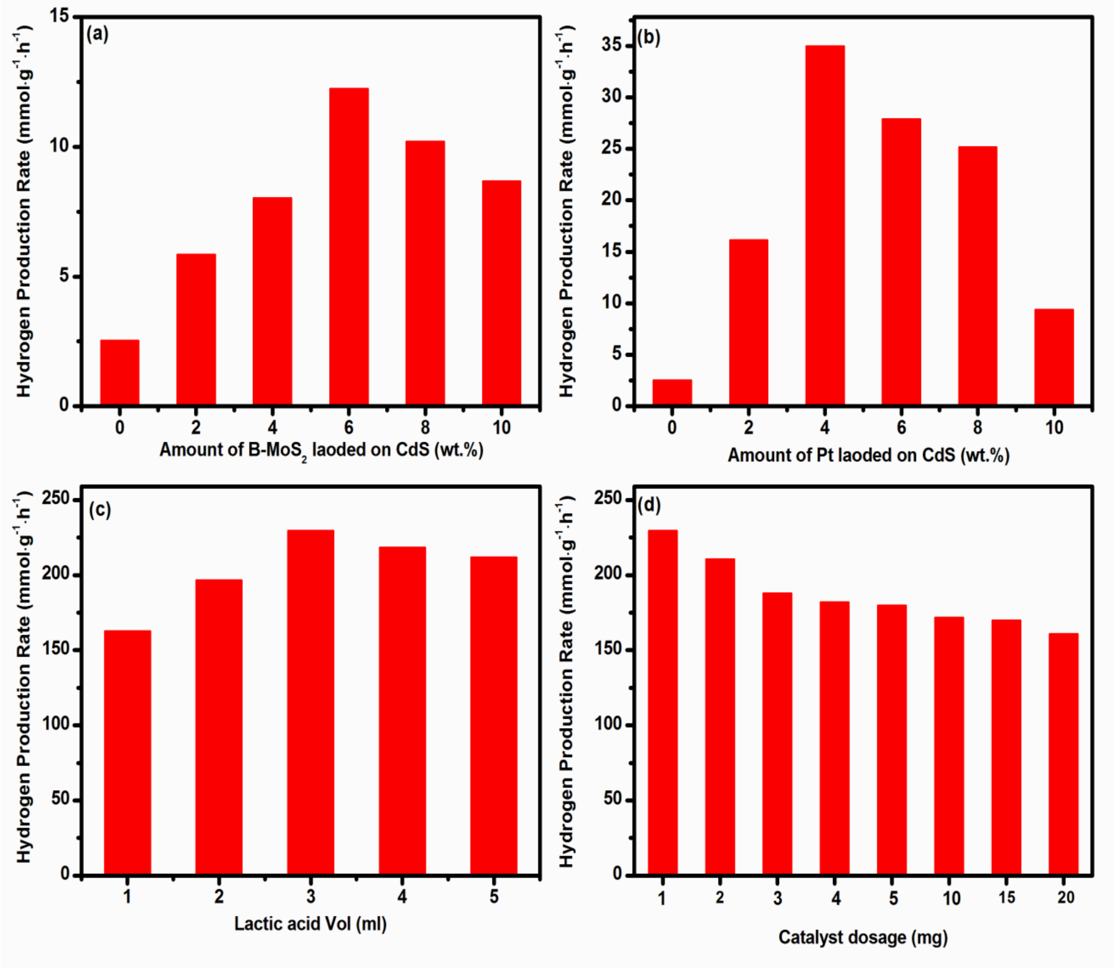

Figure S13. Hydrogen production rate in a 15-mL aqueous solution containing lactic acid 20 % with suspended (a) CdS/B-MoS$_2$, (b) CdS/Pt, nanocomposites (1 mg) containing 0, 2, 4, 6, 8, and 10 wt.% of B-MoS$_2$, and Pt, respectively. (c) Effect of sacrificial lactic acid concentration on the hydrogen evolution rate (photocatalyst: CdS/HUT-MoS$_2$-1 nanocomposite; photocatalyst dose: 1 mg; time: 5 h). (d) Effect of photocatalyst dose on hydrogen production rate (photocatalyst: CdS/HUT-MoS$_2$-1 nanocomposite; photocatalyst dose: 1, 2, 3, 4, 5, 10, 15 and 20 mg; time: 5 h).

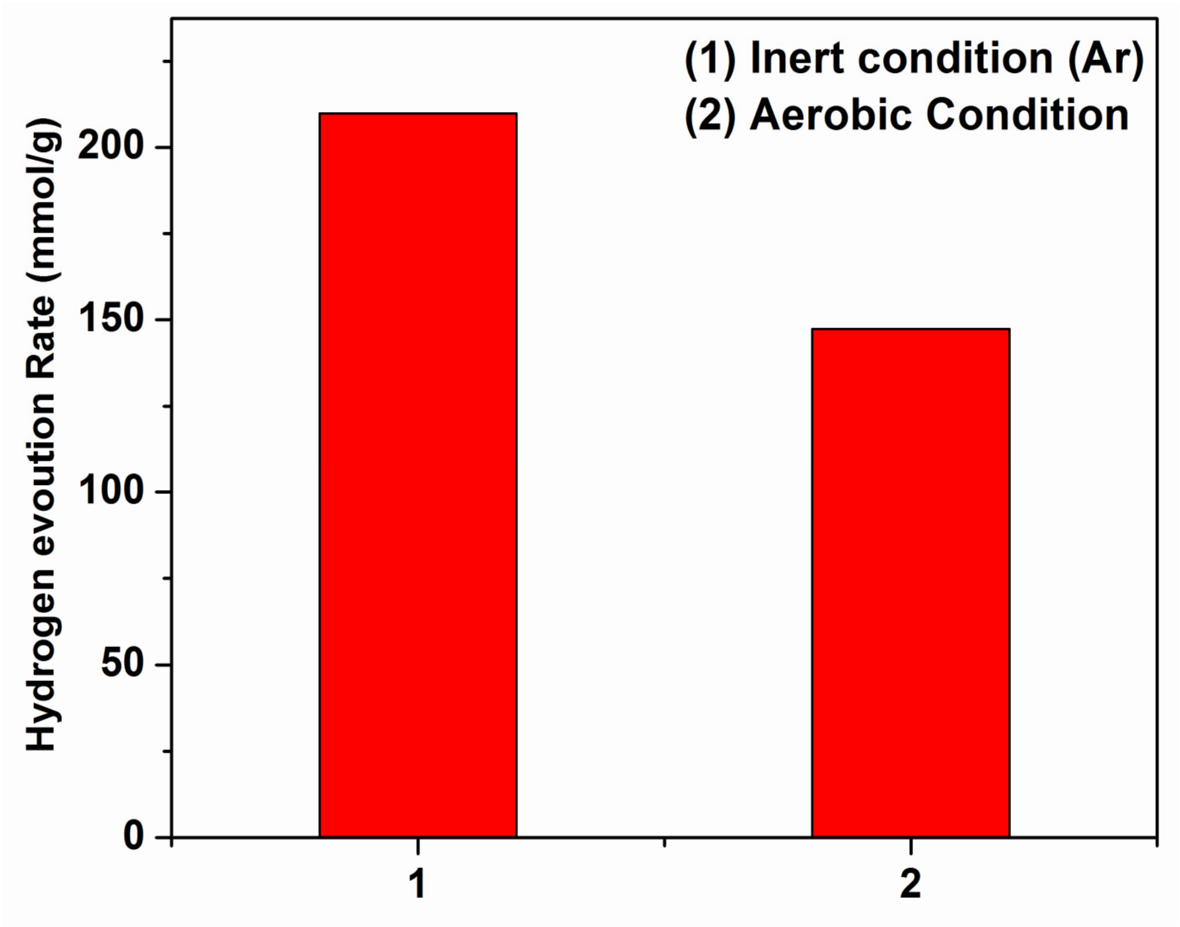

Figure S14. Photocatalytic hydrogen evolution rate of CdS/HUT-MoS$_2$ nanostructures (1) under inert condition (2) under aerobic conditions.

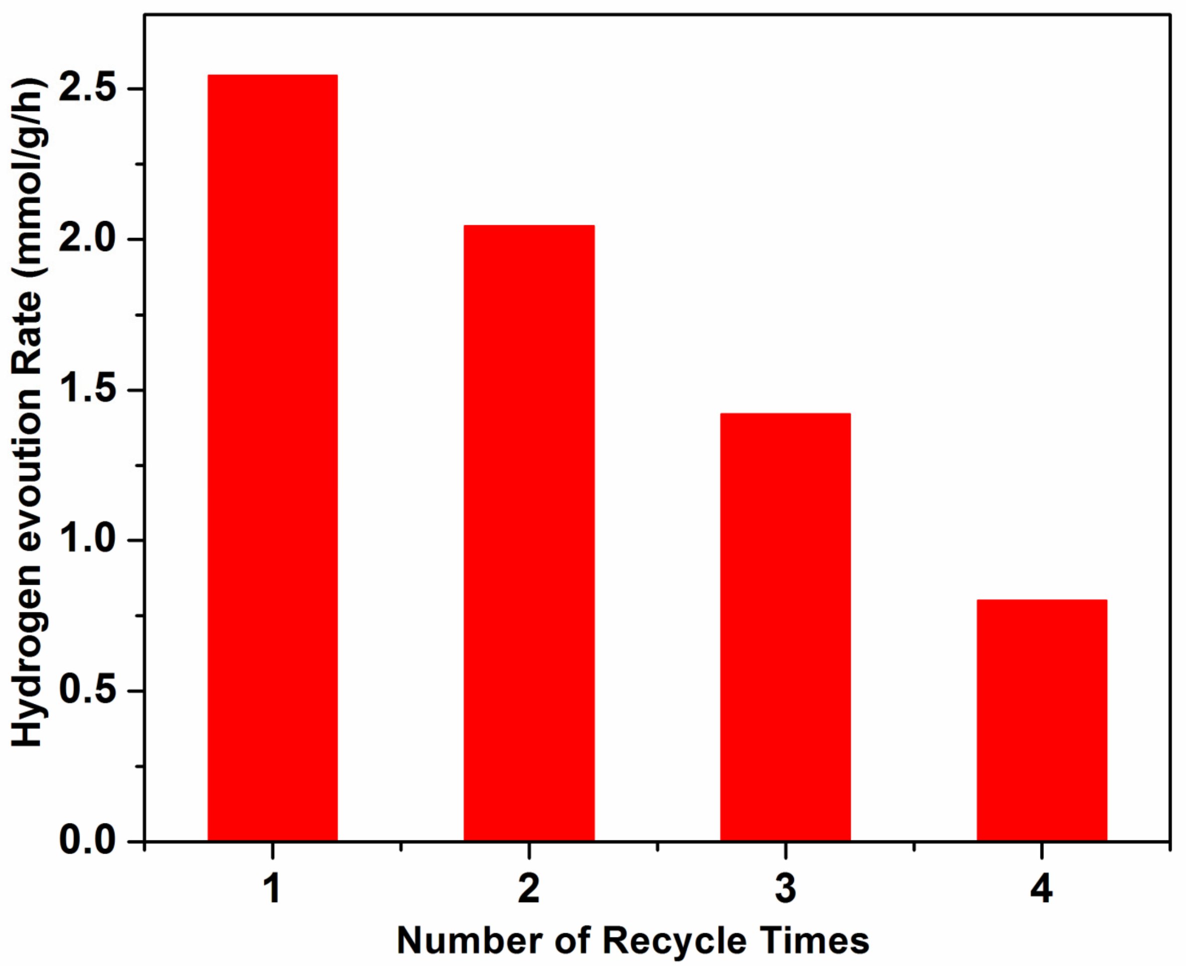

Figure S15. Recycling measurement of hydrogen production using the as-synthesized CdS nanostructures.

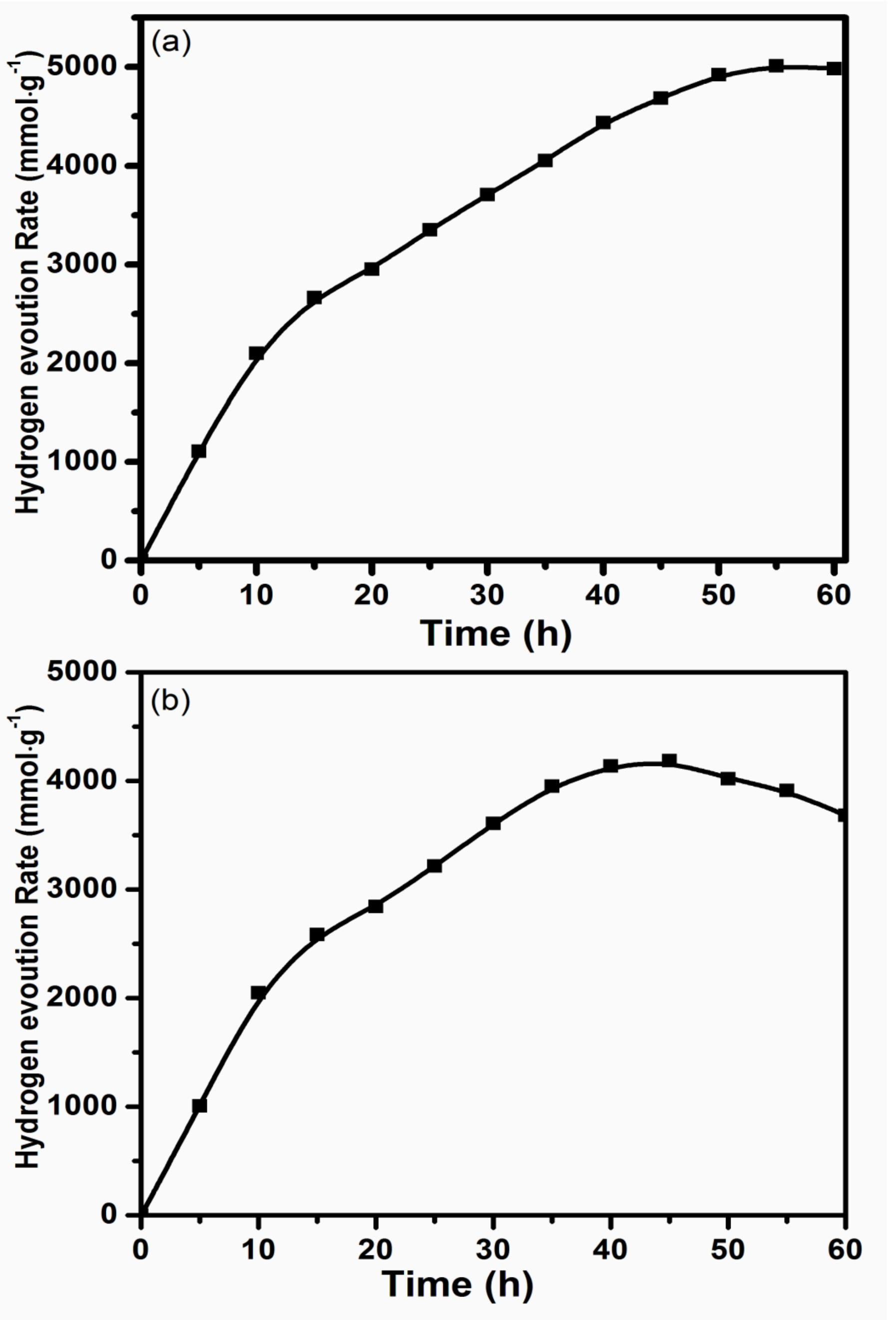

Figure S16. (a) Long-term stability test of hydrogen evolution over the optimized CdS/MoS_2-HUT-1 nanocomposite under Ar. (b) Long-term stability of CdS/HUT-MoS_2 after degassing photocatalytic reactor.

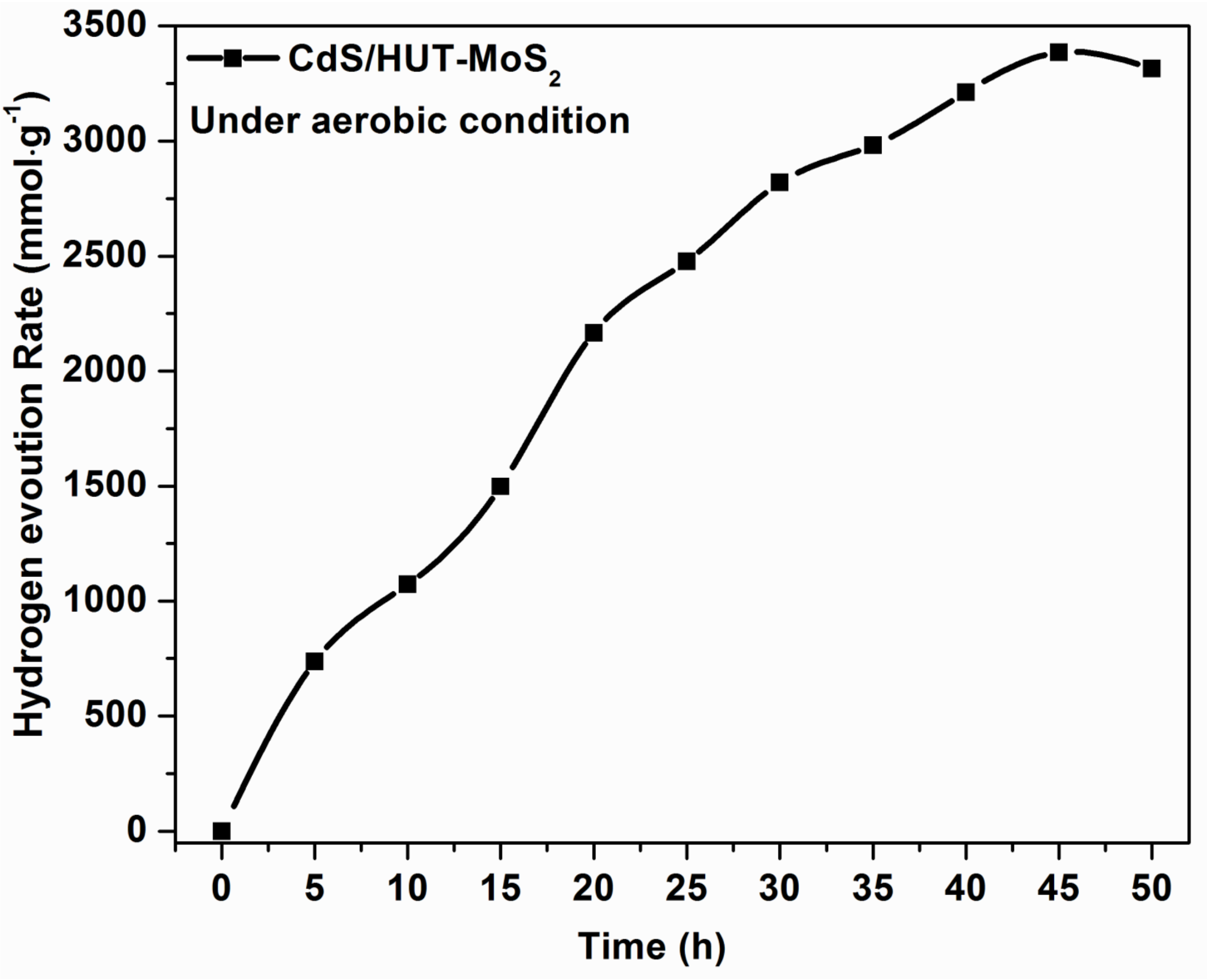

Figure S17. Long-term stability test of hydrogen evolution over the optimized CdS/MoS_2-HUT-1 nanocomposite under aerobic conditions.

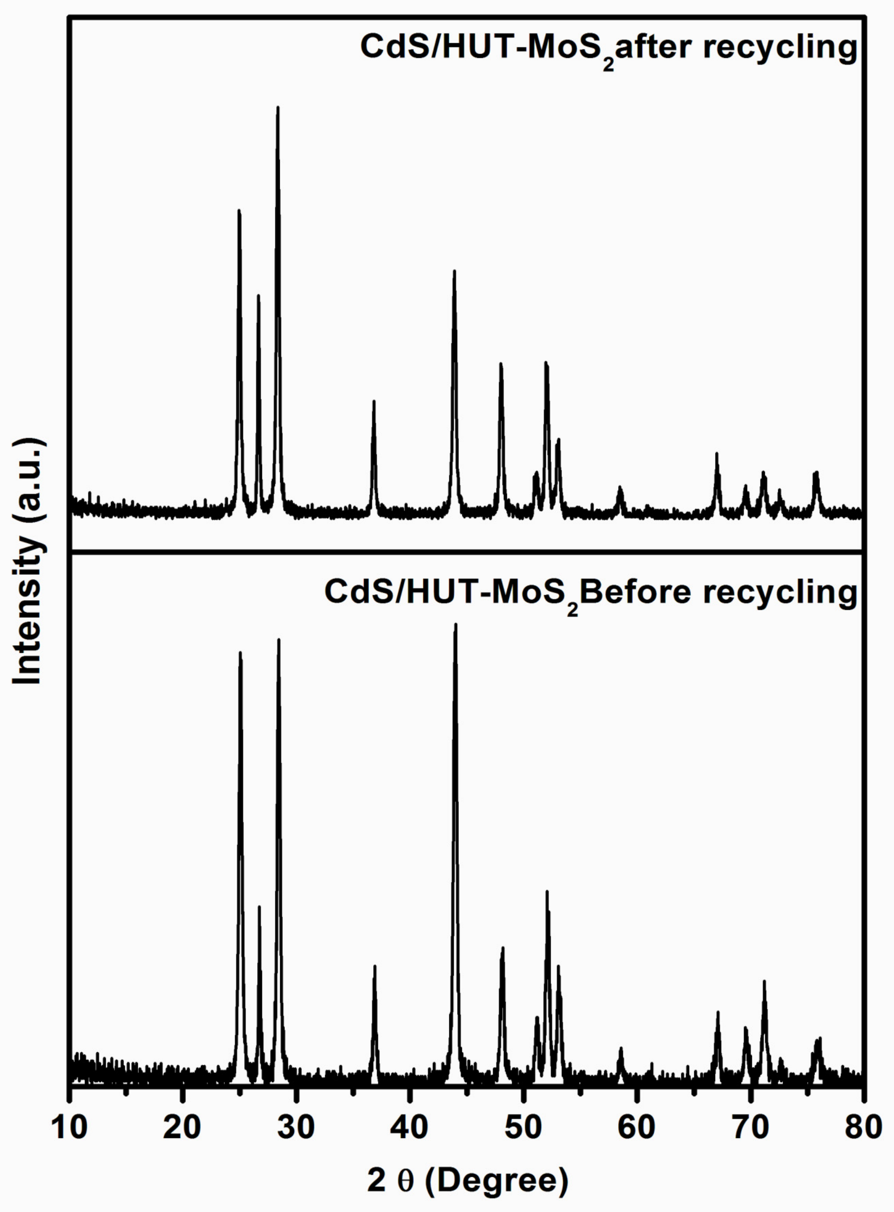

Figure S18. The XRD patterns of CdS/HUT-MoS_2 nanocomposite before and after photocatalytic recycling measurement.

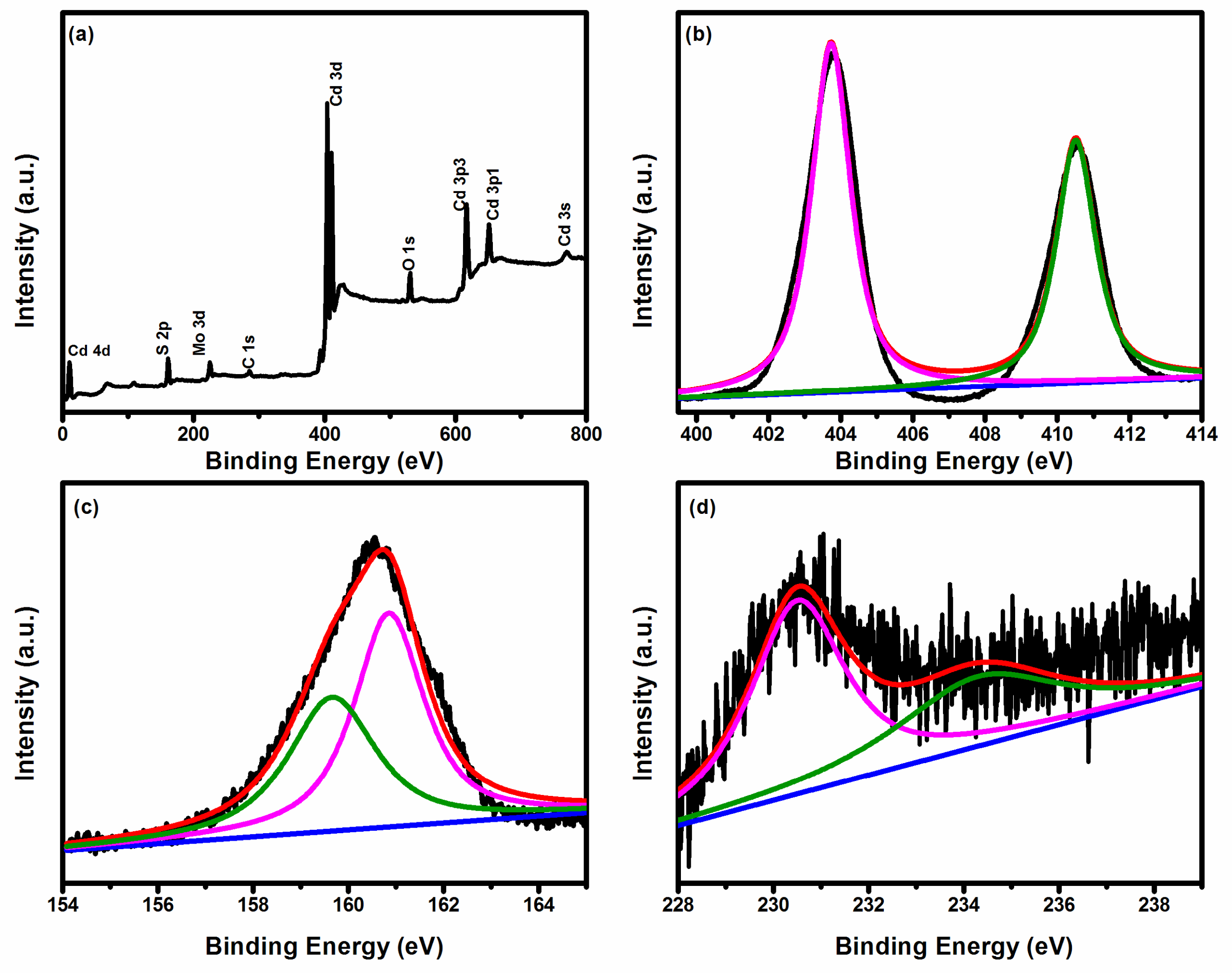

Figure S19. The XPS patterns of CdS/HUT-MoS_2 nanocomposite after photocatalytic recycling measurement: (a) survey spectrum and (b-d) narrow scan XPS spectra of Cd 3d, S 2p and Mo 3d respectively.

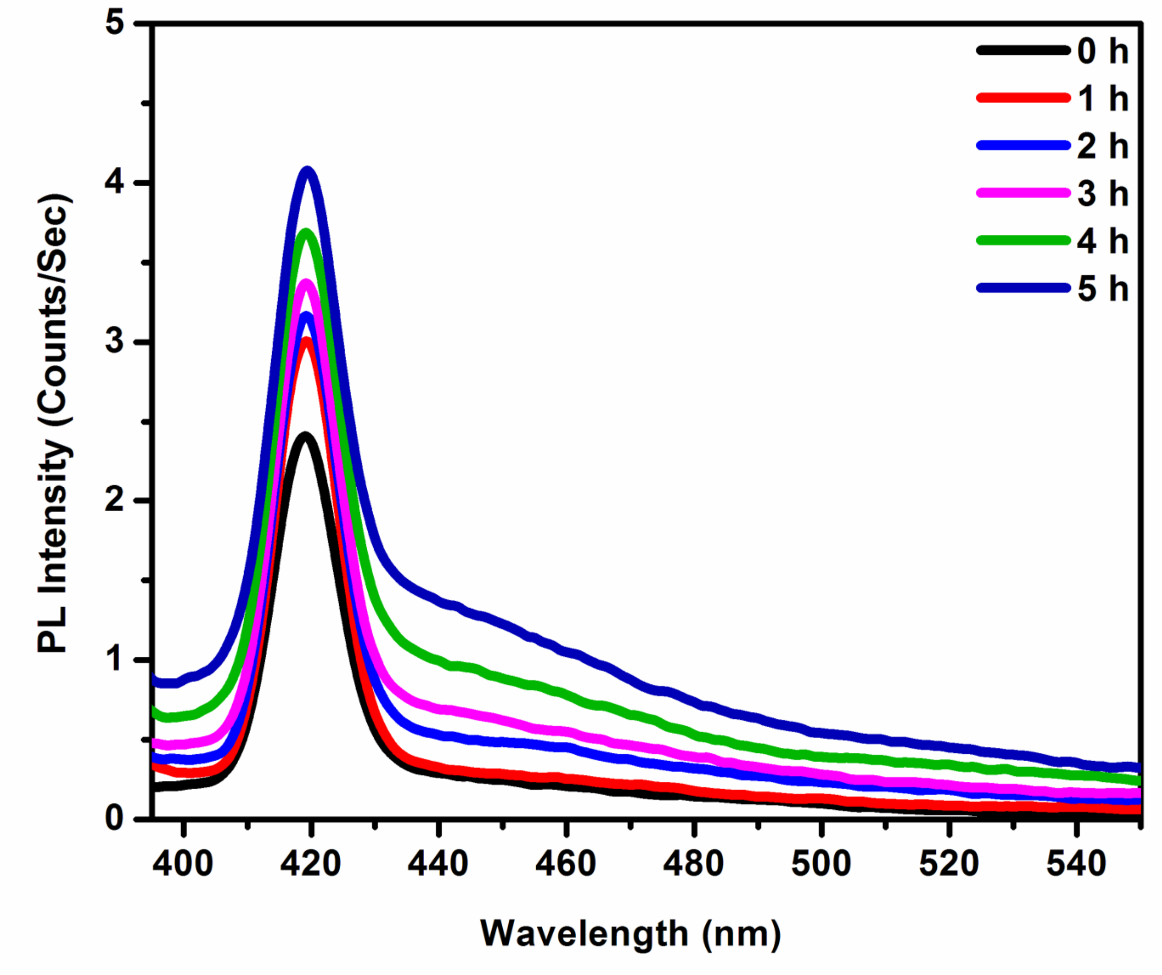

Figure S20. The terephthalic acid (TA) PL approach to know the OH radicals produced during the photocatalytic reaction process using CdS/HUT-MoS_2 nanocomposite under simulated sunlight irradiation.

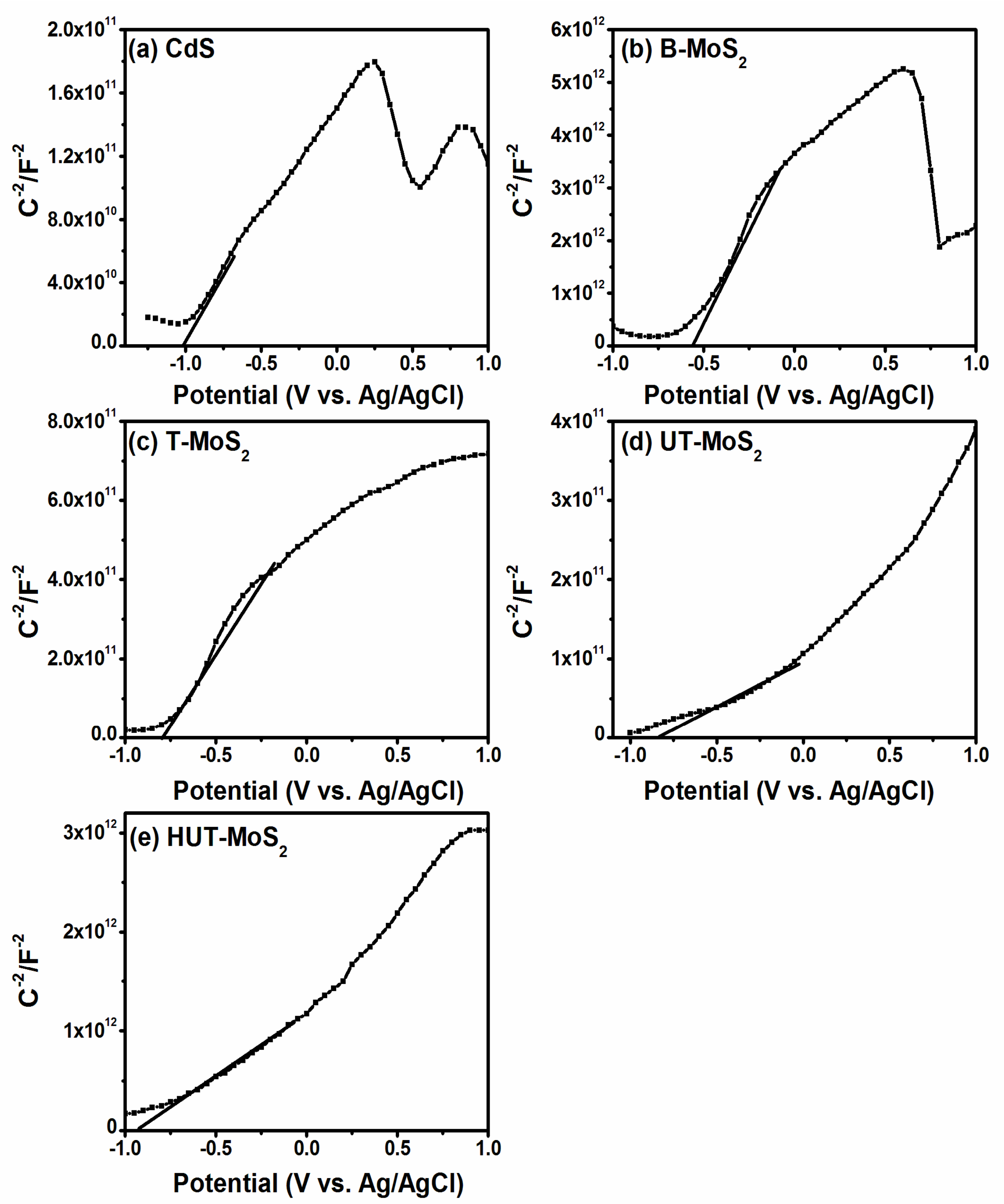

Figure S21. Mott-Schottky plots of (a) CdS nanorods, (b) B-MoS$_2$, (c) T-MoS$_2$ (d) UT-MoS$_2$ and (e) HUT-MoS$_2$ nanostructures.

Table S1. Comparison of photocatalytic H_2 evolution rate reported in the literature using MoS_2 based nanostructures as a co-catalyst on CdS nanostructures with our present results

Photocatalyst	**Catalyst Amount (mg)**	**Scavenger**	**Light Source**	**Hydrogen Evolution Rate (mmol/g/h)**	**QE (%)**	**Ref.**
CdS/HUT-MoS_2	**1**	**Lactic acid**	**Natural Sunlight** **AM 1.5G** **150 W Xe lamp ($\lambda > 425$ nm)**	**238** **209** **142**	**53.3**	**This Study**
CdS/Ag-MoS_2 CdS/Cr-MoS_2 CdS/MoS_2	10	Na_2S + Na_2SO_3	300 W Xe lamp ($\lambda > 420$ nm)	107 38 18	-	S1
CdS/UT-MoS_2	20	Lactic acid	300 W Xe lamp ($\lambda > 400$ nm)	95.7	46.9	S2
CdS/N-RGO-MoS_2, CdS/SL-MoS_2	30	Lactic acid	Solar simulator (150 W Xe lamp)	52.66 30.0	-	S3
CdS/MoS_2	200	Lactic acid	300 W Xe lamp ($\lambda > 420$ nm)	49.80	41.37	S4
CdS/UiO-66/MoS_2	20	Lactic acid	300 W Xe lamp ($\lambda > 420$ nm)	32.5	23.6	S5
CdS/MoS_2	100	Lactic acid	300 W Xe lamp ($\lambda > 400$ nm)	13.4	-	S6
CdS/UT-MoS_2	1	Lactic acid	Natural sunlight	174	38.7	S7
CdS/MoS_2-RGO CdS/MoS_2	50	Lactic acid	350 W Xe lamp ($\lambda > 420$ nm)	12.426 11.026	54.4 31.8	S8
CdS/MoS_2/RGO	200	Lactic acid	300-W Xe ($\lambda > 420$ nm)	9.0	28.1	S9
CdS/MoS_2/RGO/CoP	1	Lactic acid	Solar simulator (150 W Xe lamp)	83.907	22.5	S10

CdS/MoS$_2$/MWCNTs	20	Lactic acid	300 W Xe lamp ($\lambda > 400$ nm)	0.676	-	S11
CdS/MoS$_2$/In$_2$S$_3$	50	Lactic acid	300 W Xe lamp ($\lambda > 420$ nm)	0.6258	-	S12
CdS/MoS$_2$	200	Lactic acid	300 W Xe lamp ($\lambda > 420$ nm)	60.28	50.07	S13
CdS/1T-MoS$_2$	20	Lactic acid	300 W Xe lamp ($\lambda > 420$ nm)	39.746	-	S14
CdS/MoS$_2$–TaON	200	Na$_2$S + Na$_2$SO$_3$	300 W Xe lamp ($\lambda > 420$ nm)	3.142	-	S15
CdS/MoS$_2$/SiW$_{11}$Co	100	Lactic acid	300 W Xe lamp ($\lambda > 420$ nm)	17.0	-	S16
CdS/MoS$_2$/ SiW$_{12}$@UiO-67	100	Lactic acid	300 W Xe lamp ($\lambda > 420$ nm)	12.7	-	S17
CdS/MoS$_2$	20	Na$_2$S + Na$_2$SO$_3$	300 W Xe lamp ($\lambda > 420$ nm)	9.7		S18
CdS/Co-MoS$_2$				20.9		
CdS/Ni-MoS$_2$				24.0	17.3	
CdS/MoS$_2$	200	Lactic acid	300 W Xe lamp ($\lambda > 420$ nm)	21.4	57.2	S19

References

[S1] L. Yang, D. Zhong, J. Zhang, Z. Yan, S. Ge, P. Du, J. Jiang, D. Sun, X. Wu, Z. Fan, S. A. Dayeh and B. Xiang, *ACS Nano*, 2014, **8**, 6979–6985.

[S2] J. He, L. Chen, F. Wang, Y. Liu, P. Chen, C. T. Au and S. F. Yin, *ChemSusChem*, 2016, **9**, 624 –630.

[S3] K. Zhang, W. Kim, M. Ma, X. Shi and J. H. Park, *J. Mater. Chem. A*, 2015, **3**, 4803–4810.

[S4] X. L. Yin, L. L. Li, W. J. Jiang, Y. Zhang, X. Zhang, L. J. Wan and J. S. Hu, *ACS Appl. Mater. Interfaces*, 2016, **8**, 15258−15266.

[S5] L. Shen, M. Luo, Y. Liu, R. Liang, F. Jing and L. Wu, *Appl. Catal. B*, 2015, **166–167**, 445–453.

[S6] M. Liu, F. Li, Z. Sun, L. Ma, L. Xu and Y. Wang, *Chem. Commun.*, 2014, **50**, 11004–11007.

[S7] D. P. Kumar, S. Hong, D. A. Reddy and T. K. Kim, *J. Mater. Chem. A*, 2016, **4**, 18551–18558.

[S8] D. Lang, T. Shen and Q. Xiang, *ChemCatChem*, 2015, **7**, 943–951.

[S9] K. Chang, Z. Mei, T. Wang, Q. Kang, S. Ouyang and J. Ye, *ACS Nano*, 2014, **8**, 7078–7087.

[S10] D. A. Reddy, J. Choi, S. Lee, Y. Kim, S. Hong, D. P. Kumar and T. K. Kim, *Catal. Sci. Technol.*, 2016, **6**, 6197–6206.

[S11] W. K. Jo and N. C. S. Selvam, *Appl. Catal. A*, 2016, **525**, 9–22.

[S12] W. Jiang, Y. Liu, R. Zong, Z. Li, W. Yao and Y. Zhu, *J. Mater. Chem. A*, 2015, **3**, 18406–18412.

[S13] X. L. Yin, G. Y. He, B. Sun, W. J. Jiang, D. J. Xue, A. D. Xia, L. J. Wan and J. S. Hu, *Nano Energy*, 2016, **28**, 319–329.

[S14] P. Du, Y. Zhu, J. Zhang, D. Xu, W. Peng, G. Zhang, F. Zhang and X. Fan, *RSC Adv.*, 2016, **6**, 74394–74399.

[S15] Z. Wang, J. Hou, C. Yang, S. Jiao and H. Zhu, *Chem. Commun.*, 2014, **50**, 1731–1734.

[S16] M. Liu, F. Li, Z. Sun, L. Xu, Y. Song and A. Munventwali, *RSC Adv.*, 2015, **5**, 47314–47318.

[S17] Y. Bu, F. Li, Y. Zhang, R. Liu, X. Luo and L. Xu, *RSC Adv.*, 2016, **6**, 40560–40566.

[S18] X. Ma, J. Li, C. An, J. Feng, Y. Chi, J. Liu, J. Zhang and Y. Sun, *Nano Res.*, 2016, **9**, 2284–2293.

[S19] X. Hai, K. Chang, H. Pang, M. Li, P. Li, H. Liu, L. Shi and J. Ye, *J. Am. Chem. Soc.*, 2016, **138**, 14962–14969.